Aquat Ecol (2020) 54:119–135
https://doi.org/10.1007/s10452-019-09730-3

Viability of pico- and nanophytoplankton in the Baltic Sea during spring

Mari Vanharanta · Samu Elovaara · Daniel J. Franklin · Kristian Spilling · Tobias Tamelander

Received: 8 May 2019 / Accepted: 29 October 2019 / Published online: 11 November 2019

Abstract Phytoplankton cell death is an important process in marine food webs, but the viability of natural phytoplankton communities remains unexplored in many ecosystems. In this study, we measured the viability of natural pico- and nanophytoplankton communities in the central and southern parts of the Baltic Sea (55°21′ N, 17°06′ E–60°18′ N, 19°14′ E) during spring (4th–15th April 2016) to assess differences among phytoplankton groups and the potential relationship between cell death and temperature, and inorganic nutrient availability. Cell viability was determined by SYTOX Green cell staining and flow cytometry at a total of 27 stations representing differing hydrographic regimes. Three general groups of phytoplankton (picocyanobacteria, picoeukaryotes, and nanophytoplankton) were identified by cytometry using pigment fluorescence and light scatter characteristics. The picocyanobacteria and picoeukaryotes had significantly higher cell viability than the nanophytoplankton population at all depths throughout the study area. Viability correlated positively with the photosynthetic efficiency (F_v/F_m, maximum quantum yield of photosystem II) as measured on the total phytoplankton community. However, an anticipated correlation with dissolved organic carbon was not observed. We found that the abiotic factors suggested to affect phytoplankton viability in other marine ecosystems were not as important in the Baltic Sea, and other biotic processes, e.g. processes related to species succession could have a more pronounced role.

Keywords Baltic Sea · Spring bloom · Phytoplankton viability · Flow cytometry · SYTOX Green

Handling Editor: Télesphore Sime-Ngando.

Electronic supplementary material The online version of this article (https://doi.org/10.1007/s10452-019-09730-3) contains supplementary material, which is available to authorized users.

M. Vanharanta (✉) · S. Elovaara · T. Tamelander
Tvärminne Zoological Station, University of Helsinki, 10900 Hanko, Finland
e-mail: mari.vanharanta@environment.fi

M. Vanharanta · S. Elovaara · K. Spilling
Marine Research Centre, Finnish Environment Institute, 00790 Helsinki, Finland

D. J. Franklin
Department of Life and Environmental Sciences, Bournemouth University, Poole BH12 5BB, UK

Introduction

Grazing by zooplankton and sinking have traditionally been considered the main loss processes for phytoplankton populations. Cell death is a third loss factor, but its quantification in marine systems, and aquatic systems in general, remains rare compared to the

quantification of sinking and grazing losses. Phytoplankton cell death can be caused by pathogens (Bramucci and Case 2019; Schieler et al. 2019) or physiological stress, and a handful of studies indicate that a considerable proportion of phytoplankton cells may not be viable (e.g. Brussaard et al. 1995; Veldhuis et al. 2001; Agustí 2004; Berman-Frank et al. 2004; Rychtecký et al. 2014). In addition to external factors, also cell-intrinsic factors (senescence) can result in reduced viability among phytoplankton (Veldhuis et al. 2001; Franklin et al. 2006; Bidle 2015). Microalgae can undergo programmed cell death under unfavourable environmental conditions (Berges and Falkowski 1998; Bidle and Falkowski 2004; Jiménez et al. 2009; Gallo et al. 2017). Cell death can also be induced by allelochemicals produced by other phytoplankton. For example polyunsaturated aldehydes (PUAs) produced by marine diatoms reduce growth and viability among other phytoplankton species (Casotti et al. 2005; Ribalet et al. 2007, 2014). Recently, it has been shown that also some nano- and picoplankton taxa produce PUAs (Vidoudez et al. 2011a; Morillo-García et al. 2014).

Although time-scales differ, phytoplankton cell death can result in cell lysis, thereby providing dissolved organic matter to the pelagic microbial food web (Franklin et al. 2006, Thornton 2014). The supply of DOM affects energy transfer to higher trophic levels, and therefore cell death can have an impact distinct from other population loss factors such as grazing and sinking. The way a phytoplankton cell dies thus influences the biogeochemical cycling of organic matter (Kirchman 1999). Dissolved organic carbon (DOC) is the largest reservoir of organic carbon in the ocean and plays an important role in marine ecosystems as the primary energy source for heterotrophic bacteria. DOC is therefore considered one of the main components of aquatic food webs (Packard et al. 2000; Gustafsson et al. 2014). In coastal environments, such as the Baltic Sea, DOC can have several origins, with riverine runoff often being a substantial source (Kuliński and Pempkowiak 2008; Hoikkala et al. 2015). Terrestrial DOC is mostly retained in river estuaries of the Baltic Sea and has its greatest influence on the coastal Bothnian Sea while the open-sea area of the western Gulf of Finland (GoF) and the Baltic Proper (BP) show primarily autochthonous origin of DOC (Hoikkala et al. 2015). Other minor DOC sources are sloppy feeding by phytoplankton grazers and DOC diffusion from faecal pellets (Lignell et al. 1993; Saba et al. 2011). Certain phytoplankton may also release excess dissolved organic material during growth or lose organic compounds passively into the surrounding water (Bjørrisen 1988, Thornton 2014).

Loss of phytoplankton cell viability can be caused by suboptimal trophic conditions, temperature and UV radiation (Berges and Falkowski 1998; Agustí and Duarte 2000; Agustí and Sánchez 2002; Agustí 2004; Llabrés and Agustí 2006). How phytoplankton viability is affected by varying abiotic stressors depends on the taxa; some phytoplankton have a wider tolerance range than other coexisting taxa (Alonso-Laita and Agustí 2006; Rychtecký et al. 2014). Such taxa could survive better in rapidly changing environments, whereas more sensitive taxa succumb to external stressors and show lower viability. The Baltic Sea is enriched with inorganic nutrients due to anthropogenic loading, and eutrophication is an ongoing process in most parts of the Baltic Sea (Fleming-Lehtinen et al. 2008). At the same time, climate change is causing structural and functional shifts in the communities of aquatic ecosystems (Li et al. 2009; Kahru et al. 2016), with potential implications for sedimentation (Tamelander et al. 2017) and biogeochemical cycles (Spilling et al. 2018) in the Baltic Sea. Patterns of group-specific phytoplankton cell viability may thus be changing as viability is affected by both abiotic factors such as inorganic nutrient availability and temperature, as well as a host of biotic factors.

Phytoplankton cell viability is poorly understood in marine environments and has not been investigated in the Baltic Sea. The aim of this study was to increase our understanding of how pico- and nanophytoplankton viability varies spatially in the Baltic Sea and to elucidate its relationship to phytoplankton community composition, physiological state (as assessed by measurements of photosynthetic efficiency) and a range of abiotic factors. We focused on the pico- and nanophytoplankton because of their importance to overall productivity, and because cell populations which mostly correspond to these size classes could be easily determined with flow cytometry allowing for rapid assessment of abundance and viability. Speed and efficiency were essential for successful viability measurement from multiple depths per site.

The specific objectives were to identify (1) potential differences in the viability of different

phytoplankton groups, and (2) test for correlations between cell viability and abiotic and biotic factors including temperature, nutrient concentration, DOC concentration (that is affected by the release from lysing phytoplankton cells), abundance of larger phytoplankton (especially diatoms as potential PUA producers) and photosynthetic efficiency (F_v/F_m) of the phytoplankton community.

Materials and methods

Field sampling

Water samples were collected during a research cruise (CFLUX16) with the R/V Aranda from 4th to 15th April 2016. The objectives of the cruise were to study the phytoplankton community composition and its effect on biogeochemical cycling of nutrients and to investigate the salt water influx. Samples were taken at a total of 26 stations in the Baltic Sea, 2 in the GoF, 20 in the BP and 4 in the Åland Sea (ÅS) (Fig. 1). Two samplings were done at station LL7S in the GoF at different times, the first time on the first day of the cruise and the second time 11 days later, on the last day of the cruise.

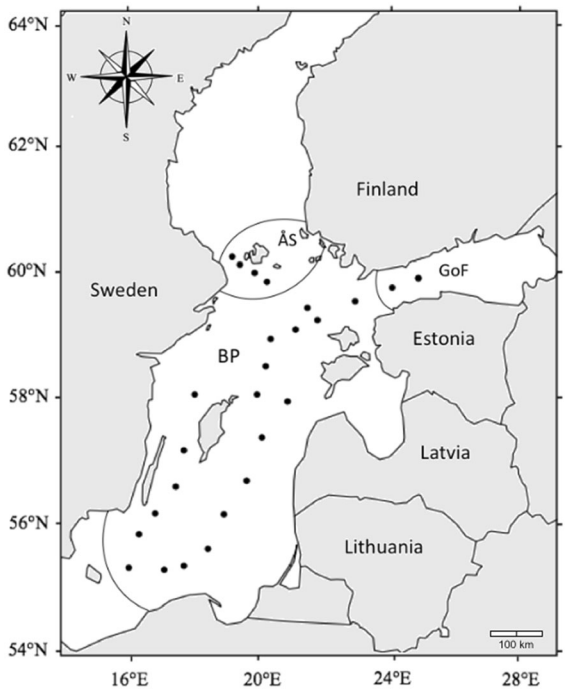

Fig. 1 Sampling sites of the CFLUX16 cruise between 4th April and 15th April 2016 at different sea areas: the Gulf of Finland (GoF), the Åland Sea (ÅS) and the Baltic Proper (BP)

Seawater samples were collected using Niskin bottles on a Rosette sampler in combination with a SeaBird SBE911 Plus CTD probe. Samples from 3 m depth were taken at every station. To examine the depth variation of phytoplankton communities, depth profiles from 19 stations were sampled at 1, 3, 10, 30 and 60 m (GoF and BP) and from 3, 10, 20 and 50 m (ÅS) (Supplementary Table 1). Water temperature, salinity, and concentrations of chlorophyll *a* (Chl *a*), inorganic nutrients ($NO_3^- + NO_2^-$, NH_4^+, PO_4^{3-}) and DOC were measured at each station. Photic zone depth was calculated from Secchi depth according to Luhtala and Tolvanen (2013).

Chl *a* concentration was determined by filtration in duplicates onto GF/F filters (Whatman). The Chl *a* was extracted in 10 mL ethanol (Jespersen and Christoffersen 1987) and stored in a freezer (− 20 °C). Samples were placed at room temperature for 24 h to ensure that all Chl *a* was extracted before measurement with a fluorescence spectrophotometer using 450 nm excitation and 670 nm emission wavelength with 10 nm slit with (Cary Eclipse, Agilent Technologies) calibrated against Chl *a* standards (Sigma-Aldrich) by linear regression ($n = 6$).

Inorganic nutrients, $NO_3^- + NO_2^-$, NH_4^+ and PO_4^{3-}, were determined using standard colorimetric methods (Grasshoff et al. 1983) directly after sampling. Limits for accurate measurements were 0.1 µmol L^{-1} for $NO_3^- + NO_2^-$ and NH_4^+, and 0.05 µmol L^{-1} for PO_4^{3-}. The DOC samples (20 mL) were filtered through 0.2-µm polycarbonate syringe filters into acid washed and pre-combusted vials, then 80 µL of 2 M HCl was added and the vials placed in a freezer (− 20 °C). The samples were placed at room temperature overnight before the DOC was determined by a high-temperature catalytic oxidation (HTCO), using a Shimadzu TOC-V CPH carbon and nitrogen analyser (Benner et al. 1993).

For microscopy, 200 mL was preserved with acidic Lugol's solution and prepared using the settling method of Utermöhl (1958). Samples were enumerated under an inverted microscope (Leitz DM IRB), and a defined area of the counting chamber was viewed at three different magnifications (125 ×, 250 ×, 500 ×). The software EnvPhyto phytoplankton counting program was used and the data stored

directly into the Hertta database (Finnish Environment Institute, Helsinki). Calculations of abundance, biovolume and carbon biomass were done automatically by the software according to Olenina et al. (2006), the biovolume list of HELCOM Phytoplankton Expert Group (PEG) (http://helcom.fi/helcomat-work/projects/phytoplankton) and Menden-Deuer and Lessard (2000).

A more detailed description of the phytoplankton enumeration method can be found in Lipsewers and Spilling (2018). Microscopy was used for determining phytoplankton community composition, whereas flow cytometry was used for counting the small phytoplankton and for dividing them into size categories (see below).

The photochemical efficiency, the ratio between variable and maximum Chl *a* fluorescence (F_v/F_m), was determined for all samples after dark acclimation (15 min) using the fluorescence induction (OJIP) curve (AquaPen fluorometer, Photon Systems Instruments) with 450 nm excitation light.

Flow cytometric analyses

Phytoplankton enumeration and viability assessment were conducted with flow cytometry (Partec Cube 8, Sysmex Partec GmbH, Goerlitz, Germany). Flow cytometry allowed the analysis of multiple depths rapidly after sampling and thereby minimized the artefacts potentially generated by sample storage, i.e. enclosure effects. Microscopic analysis of viability would not have been possible within the schedule of the cruise. Flow cytometry allows for easy and detailed analysis of pico- and nano-sized phytoplankton that are difficult to analyse microscopically.

The seawater samples were kept cold (in situ temperature) in darkness until they were split into subsamples for flow cytometric measurements. These measurements were conducted within 1 to 7 h (on average 2 h 27 min) after sampling, except for a 9 h delay at BY32 and BY15 due to harsh weather conditions. In total, four subsamples of 800 µL were taken from each sampling depth to determine phytoplankton cell viability and cell abundance. One of the four subsamples was kept unstained to estimate the green background fluorescence, and the other three were stained with 4 µL SYTOX Green to a final concentration of 0.5 µM (Veldhuis et al. 2001). The stained and gently mixed subsamples were incubated in cold and dark from 10 min (minimum staining time based on recommendations of manufacturer) to 30 min prior to flow cytometry measurements. Viability did not differ systematically between samples measured after 10 and 30 min suggesting that the stain incorporation within this time range was uniform (data not shown).

Abundance and viability of pico- and nanophytoplankton were determined with the flow cytometer equipped with two Argon lasers (488 and 561 nm excitation light). A threshold of 0.001 arbitrary units on forward scatter was used to exclude instrument noise and small particles. Three groups of small unicellular phytoplankton (Fig. 2a) were identified based on forward scatter and orange fluorescence (610/30 bandpass filter) according to previous flow cytometric, phytoplankton studies (Olson et al. 1993; Smith 2009; Tarran and Bruun 2015). The first group (G1) included cells with low forward scatter and high orange fluorescence (phycoerythrin) and was assumed to contain mostly picocyanobacteria. The second group (G2) included cells with comparable forward scatter but lower orange fluorescence and was considered to contain most of the picoeukaryotes. Cells in the third group (G3) expressed intermediate to high orange fluorescence and higher forward scatter than the two previous groups and were assumed to contain larger cells mostly consisting of nanophytoplankton. The sample flow rate was 2 µL per second, and the counted volume was 200 µL. Flow cytometric data were analysed with FCS Express 5 software (De Novo Software). As the green fluorescence (536/40 bandpass filter) increases in stained non-viable cells, the viability (%) of each sample was determined as the ratio of non-stained cells to all counted cells (Fig. 2e–i). Similar to the recent approach used by Rychtecký et al. (2014) in an analysis of freshwater phytoplankton, cells were considered non-viable if their green fluorescence signal exceeded the green autofluorescence of the unstained sample (Fig. 2d) by at least fivefold (Veldhuis et al. 2001; Timmermans et al. 2007). The percentage of viable cells was assessed when the cell abundance of all subsamples exceeded 100 cells per sample volume (200 µL). Smaller cell numbers were found to be subject to strong variability and potential outliers and were consequently excluded from further analysis.

A major uncertainty associated with SYTOX Green staining, as well as with most cellular stains, is that

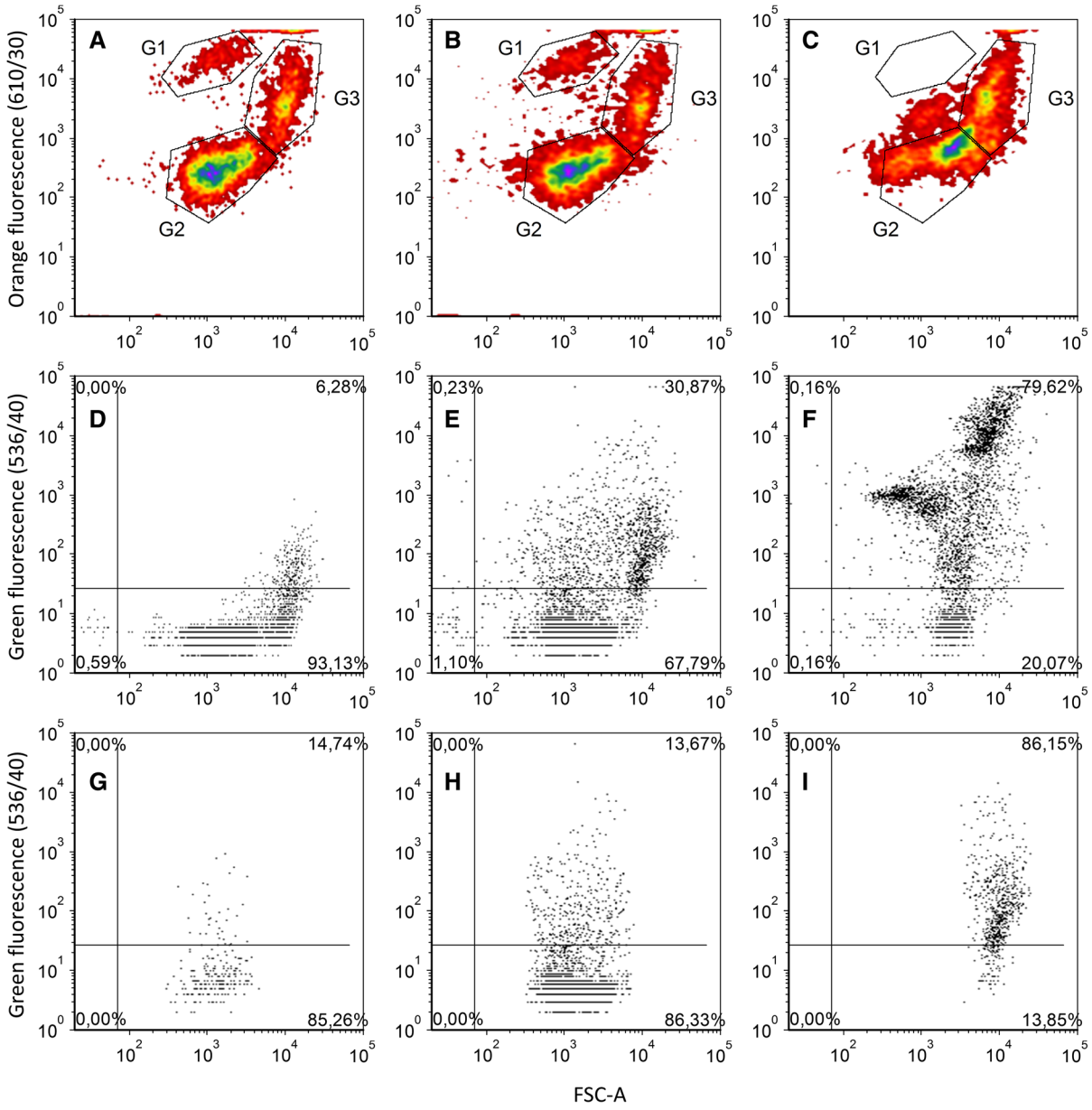

Fig. 2 Density plots showing the three groups of phytoplankton cells (G1, G2 and G3) detected by phycoerythrin (orange fluorescence (610/30)) and forward-scattered light (FSC) signals in unstained (**a**), SYTOX Green stained (**b**), and stained and heat-killed (**c**) samples. Green autofluorescence in unstained sample (**d**). Determination of SYTOX Green stained cells (upper quadrants) in fresh (**e**), and heat-killed samples (**f**). Viable cells in lower quadrants (**e** and **f**). **g–i**: Determination of viable cells (lower quadrants) in SYTOX Green stained samples for G1, G2 and G3, respectively. Examples are from 3 m depth at station LL7S in the Gulf of Finland, 15th April. (Color figure online)

uniform response among different cell types (i.e. phytoplankton species, in this case) cannot be guaranteed, as discussed by, e.g. Veldhuis et al. (2001) and Peperzak and Brussaard (2011). Therefore, we used killed control samples to assess the comprehensiveness of SYTOX Green staining within the total phytoplankton community at each site. One subsample from 3 m at each station was killed by keeping the sample tube in a hot water bath (80 °C) for 10 min. The heat-treated samples were used as a

positive control, with all cells in the sample assumed to be dead (Franklin et al. 2009). The same staining procedure described above was conducted with the heat-treated samples to test possible differences in staining intensity of the dead cells among different phytoplankton groups (Peperzak and Brussaard 2011). Heat-treating altered the scatter and fluorescence properties of the cells (Fig. 2c) in a way that they could not reliably be divided into the same groups as the non-heated samples (Fig. 2b), which prevented direct comparison of differences in staining. Therefore, we calculated the abundance ratio of each group to all other groups and to total cell abundance (flow cytometry results) in non-heated samples and compared these ratios against the viability of the heat-treated cells at each site. We also compared flow cytometry derived total abundance and Chl *a* concentration against the viability of the heat-treated cells to retrospectively test if the used SYTOX Green concentration had been sufficient to stain the maximum amount of dead cells.

Statistical analyses

All statistical analyses were done using R version 3.5.1 (R Core Team 2018). Differences in viability among the three phytoplankton groups and vertical differences in viability and cell abundance of phytoplankton communities were analysed using Welch-ANOVA. A nonparametric method was chosen due to unequal sample sizes and heteroscedasticity among the three flow cytometer-based phytoplankton groups. Games–Howell post hoc test was applied on the significant Welch-ANOVA results. Before analyses, the percentage values of viability were logit transformed, which is a transformation commonly used for proportions. Differences were considered significant at a p value < 0.001. Detailed results for Welch-ANOVA tests are presented in Supplementary Table 2.

A generalized linear model (GLM) with beta distribution was used to investigate relationships between phytoplankton viability versus environmental variables and large phytoplankton (i.e. species counted with microscopy) abundance. Beta distribution was chosen because of its applicability to analysing proportions. Different model selections were conducted between viability and abiotic variables and between viability and large phytoplankton abundance to avoid collinearity issues between abiotic variables and large phytoplankton. GLM with beta distribution was also used for investigating the relationship between F_v/F_m and viability. We used a negative binomial GLM to investigate the relationship between phytoplankton abundance and environmental variables and large phytoplankton because negative binomial GLM can be used to analyse count data and to deal with overdispersion. Linear regression was used when the response variable was neither proportion nor count data. Model selection for GLM was done using Akaike information criterion. Data exploration was performed according to the protocol of Zuur et al. (2010) as closely as possible. Individual regressions were conducted for abundances and viabilities for G3 and G2, as the two groups were assumed to occupy different ecological niches. These regression models only apply to 3 m depth as deeper samples were not taken at every station. G1 were excluded from the regression analyses because this group was present in too low abundance at many stations. Stations BOSEXC1 and BY15 in the BP were excluded from the statistical analyses due to missing values of temperature and salinity at BOSEXC1 and a laboratory error in DOC measurement at BY15. Detailed regression model parameters are presented in Supplementary Table 3.

Results

Physicochemical properties of the water

Physical and chemical variables at 3 m depth of each sea area are summarized in Table 1. Temperature and salinity had a northeast-ward gradient characterized with decreasing values from the BP to the GoF. The upper limit of the halocline ranged between 50 and 70 m. NO_3^- and Chl *a* concentrations were highest in the GoF. The Chl *a* concentration was lower in the BP than in the GoF and the ÅS. A similar trend was observed with NO_3^- concentration, except for the three stations in the Western Gotland Basin that had higher NO_3^- than the other stations in the BP (Supplementary Figure 1a). PO_4^{3-} concentration was on average high in southerly stations, whereas northerly stations had high variation, with both high and low concentrations. The concentration of DOC varied between 3.8 and 23.0 mg L^{-1} at 3 m. The

Table 1 Mean values and standard deviations (± SD) of temperature (*T*) (°C), salinity (Sal), $NO_3^- + NO_2^-$ (µmol L^{-1}), NH_4^+ (µmol L^{-1}), PO_4^{3-} (µmol L^{-1}), Chl *a* (µg L^{-1}), DOC (mg L^{-1}) and photochemical efficiency (F_v/F_m) in the Gulf of Finland, the Baltic Proper, and the Åland Sea at 3 m

Sea area	*T*	Sal	$NO_3 + NO_2$	NH_4	PO_4	Chl *a*	DOC	F_v/F_m
Gulf of Finland	2.5 ± 0.6	5.1 ± 0.1	1.3 ± 2.0	0.1 ± 0.0	0.5 ± 0.1	19.6 ± 9.0	16.0 ± 9.4	0.63 ± 0.07
	(1.8–2.9)	(4.9–5.2)	(0.0–3.6)	(0.1–0.1)	(0.3–0.6)	(9.4–26.1)	(5.3–23.0)	(0.54–0.71)
Baltic proper	4.4 ± 0.8	7.0 ± 0.5	0.1 ± 0.4	0.1 ± 0.0	0.4 ± 0.1	5.9 ± 3.3	8.4 ± 2.5	0.65 ± 0.08
	(2.5–5.7)	(5.9–7.8)	(0.0–1.9)	(0.0–0.2)	(0.2–0.6)	(1.7–11.4)	(3.8–15.1)	(0.49–0.79)
Åland Sea	3.0 ± 0.2	5.6 ± 0.1	0.1 ± 0.1	0.1 ± 0.0	0.2 ± 0.0	9.2 ± 1.1	8.1 ± 2.9	0.62 ± 0.05
	(2.8–3.3)	(5.5–5.7)	(0.0–0.2)	(0.1–0.2)	(0.1–0.2)	(7.4–10.2)	(4.1–11.8)	(0.56–0.67)

The range is presented in parenthesis

highest concentration of DOC was measured in the GoF at the end of the cruise (15th April), and it was generally lower in the BP and the ÅS than in the GoF. Photosynthetic efficiency (F_v/F_m) was similar in all three sea areas. Temporal change at station LL7S in the GoF was characterized by increased surface water temperature (from 1.8 to 2.9 °C), depleted NO_3^- from the upper layer and higher Chl *a* concentration (26.1 µg L^{-1}) during the second sampling compared to the first sampling (23.5 µg L^{-1}). Calculated photic zone depth was on average 16 m with minimum and maximum depths of 11 m and 23 m, respectively.

Abundance and viability of pico- and nanophytoplankton

The total abundance of phytoplankton measured by flow cytometry was highest in the GoF and the ÅS (Supplementary Figure 1b). In general, abundance was highest in the 0–10 m photic layer and lower at 30 m (Fig. 3). An exceptionally high abundance (4.0×10^4 cells mL^{-1}) was observed in the surface water at station F67 in the ÅS. Average phytoplankton viability remained almost unchanged in the photic zone (approximately 1–10 m), decreased slightly at 30 m and was significantly lower at 60 m (Fig. 3) (Welch-ANOVA, $F(4, 36.045) = 9.8984$, $p < 0.001$).

Relative cell abundances of G1, G2 and G3, as determined by flow cytometry (Fig. 2), varied broadly across the study area (Table 2), but all three groups were most abundant in the ÅS and GoF and least

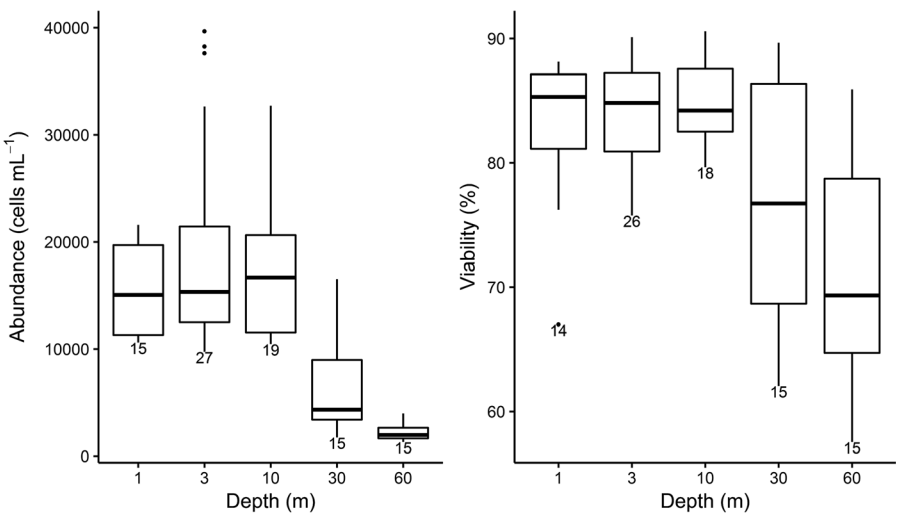

Fig. 3 Flow cytometry-based total abundance (cells mL^{-1}) (left panel) and percentage of viable cells (right panel) of phytoplankton at depths 1, 3, 10, 30, and 60 m. Sample size below each box

Table 2 Cell abundances (cells mL^{-1}) of G1, G2 and G3 in the Gulf of Finland, the Baltic Proper and the Åland Sea at depths 1, 3, 10, 20, 30, 50, 60 m

Sea area	Group	1 m	3 m	10 m	20 m	30 m	50 m	60 m
Gulf of Finland	G1	1155 ± 130	1394 ± 192	1215 ± 166	–	287 ± 37	–	365 ± 61
	G2	14,473 ± 383	21,350 ± 6617	19,571 ± 6146	–	2288 ± 527	–	1618 ± 247
	G3	3158 ± 248	3310 ± 305	2867 ± 443	–	805 ± 372	–	547 ± 196
Baltic proper	G1	211 ± 85	302 ± 153	236 ± 130	–	161 ± 100	–	217 ± 80
	G2	10,769 ± 4228	11,390 ± 4013	11,178 ± 3649	–	4846 ± 3190	–	1495 ± 621
	G3	2043 ± 1037	1747 ± 634	1801 ± 878	–	1045 ± 984	–	269 ± 144
Åland Sea	G1	–	866 ± 99	785 ± 175	583 ± 408	–	130 ± 30	–
	G2	–	31,556 ± 2939	27,833 ± 2738	18,510 ± 12,525	–	1653 ± 413	–
	G3	–	1679 ± 323	1350 ± 110	913 ± 403	–	238 ± 28	–

Average cell count ± SD

abundant in the southernmost stations of the BP. G1 was the least abundant group at all stations. G1 was present in sufficient abundance to assess viability only at 10 of the more northerly stations. At most of the stations in the central and southern BP, G1 was either very low or almost absent. G2 was numerically dominant at all stations and sampling depths, accounting for on average 77% of the total phytoplankton abundance measured by flow cytometry at 3 m. The abundance of G3 (on average 11%) was generally smaller compared to G2, but their abundance at 3 m depth was high at some stations in the BP (5–40% of cytometry-based groups). At many stations, the abundance of G3 was too low for viability assessments at 30 m and 60 m. Community composition of large phytoplankton, as defined on class level by light microscopy, was mostly diatom dominated (Supplementary Figure 2). In GoF and ÅS also dinoflagellate biomass was high. Variation in biomass contribution per class was highest in BP where also cryptophytes occasionally reached biomass comparable to diatoms.

G2 and G3 had slightly different depth distributions (Fig. 4). G2 was most abundant in the 1–10 m photic layer and decreased at 30 m (Welch-ANOVA, $F(4, 36.323) = 48.218$, $p < 0.001$), but were regularly found also at 60 m. G3 was often abundant also at 30 m depth and decreased significantly only at 60 m (Welch-ANOVA, $F(4, 37.892) = 43.493$, $p < 0.001$), where it was much less abundant than G2.

The most noticeable difference in viability could be observed among phytoplankton groups (Fig. 5). The viability of G3 at 3 m depth was significantly lower compared to the two picophytoplankton populations

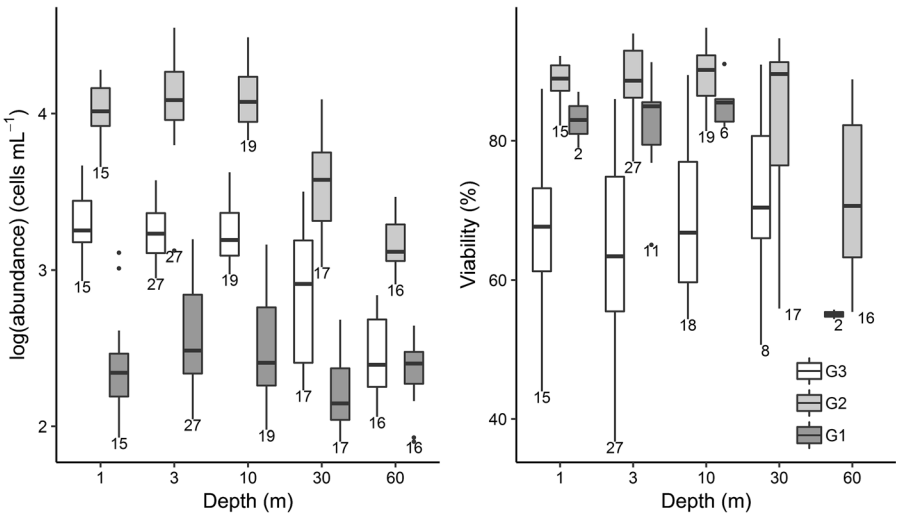

Fig. 4 G1, G2 and G3 abundance (left panel) and viability (right panel) at depths 1, 3, 10, 30, and 60 m. Sample size below each box

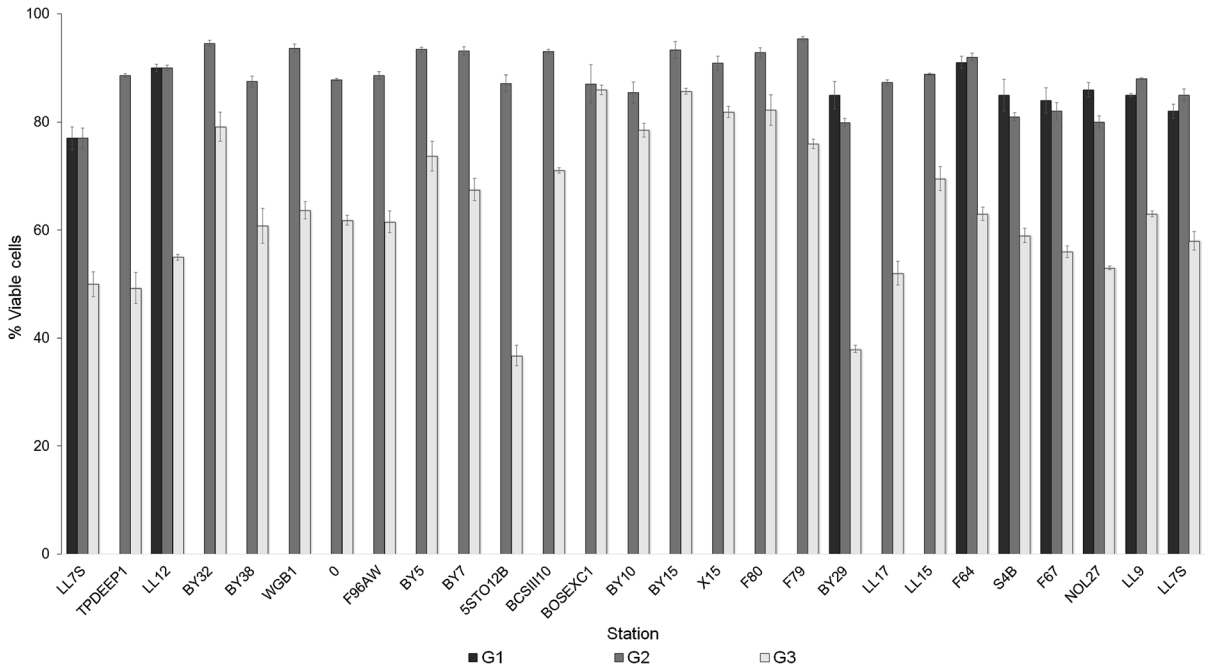

Fig. 5 Average percentage of viable cells ± SE (n = 3) of G1, G2 and G3 at 3 m depth. The station order in the horizontal axis follows the cruise route, which started and ended in the GoF (station LL7S) (see Fig. 1). Stations LL12 and BY29 were the only stations in the Baltic Proper with sufficient abundance of G1 cells for viability assessments. Therefore, G1 is missing from most of the stations in the central and southern parts of the Baltic Proper

(Welch-ANOVA, $F(2, 19.649) = 22.974$, $p < 0.001$). At 3 m depth, the viability of G3 varied between 37 and 86%, whereas the viability of G1 and G2 varied between 77 and 91%, and 77 and 95%, respectively. Percentages of viable cells of G1 and G2 were similar across the study area (Fig. 5). Mean viabilities of the pico-sized populations at 3 m depth were 85% (G1) and 88% (G2), while the mean viability of G3 was 64%. The lowest viability at 3 m depth was measured at station 5STO12B in the southern BP, where viable cells accounted for only 37% of the G3 population. The corresponding total viability of all three groups at the station 5STO12B was 76%, however. The highest viability percentage of all groups was observed at stations BY32 and F79 in the BP, where the percentage of viable cells accounted for 95% of the G2 population. G3 viability was lower than the viability of G2 also at all other sampling depths (1, 10, 30 and 60 m) (Fig. 4). G3 viability showed greater range than that of G2, but average viability did not differ significantly among the sampling depths. Due to low cell abundance, G3 viability at 60 m could only be assessed twice during the whole cruise, on the last sampling day in the GoF. G2 viability at 60 m depth was significantly lower than the viability at 1–10 m (Welch-ANOVA, $F(4, 41.344) = 10.213$, $p < 0.001$). At some stations, the 60 m sample was taken below the halocline (data not shown). The viability of G2 at 60 m at those stations was slightly lower than at stations where the halocline was deeper than 60 m (Welch-ANOVA, $F(1, 13.456) = 11.048$, $p = 0.005$). Assessment of G1 viability with depth was not possible due to low cell abundance.

G3 abundance at 3 m depth correlated positively with NH_4^+ concentration, although the relationship was not highly significant (negative binomial GLM, generalized $r2 = 0.28$, $p = 0.00113$, Fig. 6a). G2 abundance correlated negatively with temperature and PO_4^{3-} concentration (negative binomial GLM, generalized $r2 = 0.79$, $p < 0.001$, Fig. 6b, c). Optimal regression models (Supplementary Table 3) explained viability of phytoplankton rather poorly. G3 viability did not correlate with any of the measured environmental variables. G2 viability correlated with PO_4^{3-} concentration, but this relationship was quite weak (pseudo-$r2 = 0.13$, $p = 0.029$). Interestingly, viability of G3 and G2 also seemed to be higher whenever the total phytoplankton density was low (as indicated by

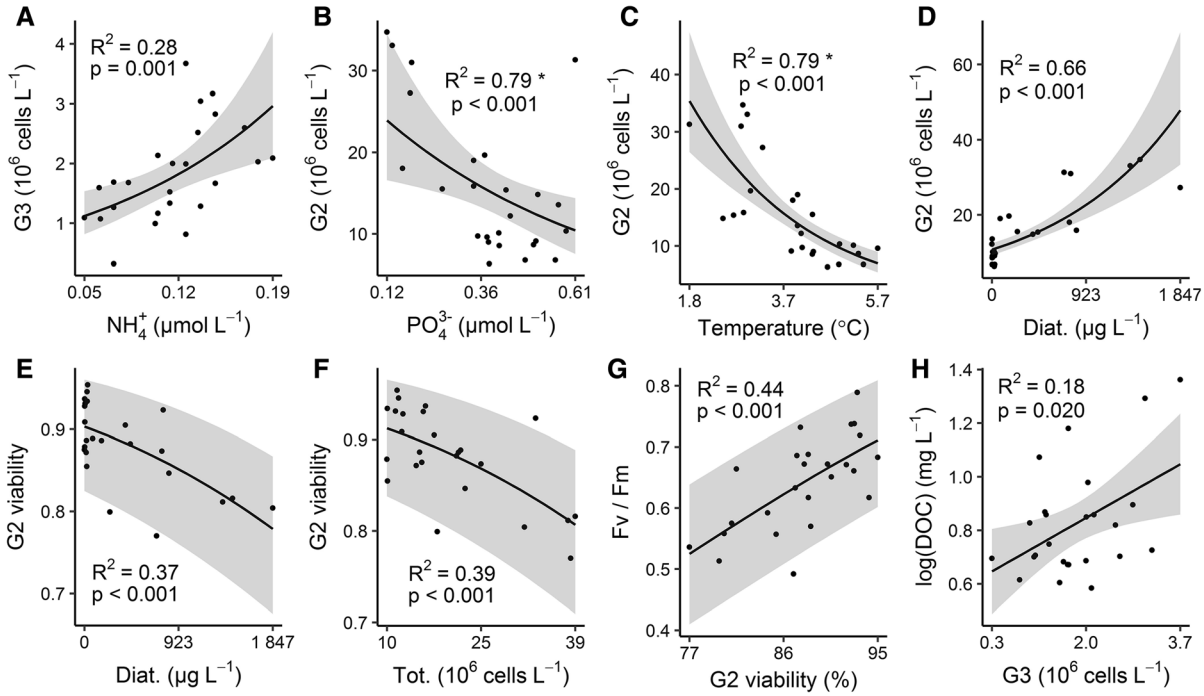

Fig. 6 Fitted values (line) and 95% confidence intervals (grey area, figures **a**–**d** and **h**) or 95% quantiles (grey area, figures **e**–**g**) of models presenting significant relationships in the data set. **a**–**d**: Negative binomial generalized linear models of the relationships between G3 and NH_4^+ (**a**), and between G2 and PO_4^{3-} (**b**), temperature (**c**) and diatom biomass (Diat.) (**d**). **e**–**g**: Beta regression models of the relationship between G2 viability and diatom biomass (**e**) and total flow cytometry-based phytoplankton abundance (Tot.) (**f**), and between F_v/F_m and G2 viability (**g**). **h**: Linear regression model of relationship between log-transformed DOC concentration and G3 abundance. Model parameters are presented in Supplementary Table 2.*Model parameters refer to a regression model containing both PO_4^{3-} and temperature. Here separated for visualization

direct flow cytometry counts and Chl *a* concentration). This was especially pronounced in the negative relationship between G2 viability and total flow cytometry-based phytoplankton abundance (beta regression, pseudo-$r2 = 0.39$, $p < 0.001$, Fig. 6f) and between G2 viability and diatom biomass (beta regression, pseudo-$r2 = 0.37$, $p < 0.001$, Fig. 6e). The latter relationship is somewhat contradictory given the positive relationship between G2 abundance and diatom biomass (negative binomial GLM, generalized $r2 = 0.66$, $p < 0.001$, Fig. 6d).

DOC concentration values were log-transformed for regression analyses to avoid issues caused by two stations with atypically high DOC concentrations. We did not find a relationship between viability and DOC, but there was a slight correlation between DOC concentration and G3 abundance (linear regression, $r2 = 0.18$, $F1, 23 = 6.28$, $p = 0.020$, Fig. 6h). The F_v/F_m correlated with G2 viability (beta regression, pseudo-$r2 = 0.44$, $p < 0.001$, Fig. 6g).

Total viability in the heat-killed samples varied from 3 to 28% with an average of 12% and standard deviation of 6%. There was no relationship between the viability in the heat-treated controls and the abundance ratios of any of the flow cytometry-based phytoplankton groups. There was a significant positive relationship between Chl *a* concentration and viability in the heat-treated controls (beta regression, pseudo-$r2 = 0.37$, $p < 0.001$, data not shown). There was no significant difference in flow cytometry total event counts between unstained and stained samples. Usually the event count in dead controls was somewhat lower than in non-heated samples and higher only at three stations. However, at these stations the event count was much higher; in particular at the station BY7 there were more than twice as many counts in the dead controls than in non-heated samples.

Discussion

The current study is to our knowledge the first to examine natural phytoplankton viability over a large spatial scale in the Baltic Sea. Total viability of the phytoplankton community measured by flow cytometry did not vary much, but our analyses revealed high variability among different phytoplankton groups and relatively low viabilities for nano-sized cells (G3). Flow cytometric studies of phytoplankton simultaneously provide information on abundance of a given size range and on the physiological state of individual cells within the community. The results from this study clearly emphasize the importance of studying viability at the single-cell level (Davey and Kell 1996), as restricting the viability analyses to the community level would have completely missed the difference in viability between pico- and nano-sized fractions.

At some stations, e.g. in the BP, non-viable cells accounted for more than half of the G3 population. The viability of G1 and G2 was significantly higher than the viability of G3, which could be a true observation or caused by different sensitivity to SYTOX Green staining between the groups. Since the total viability of the heat-killed phytoplankton samples did not differ regardless of the proportion of individual groups within the community we can cautiously assume that the staining sensitivity of all the groups is equal. Of course, this is only a very approximate test of equal staining and does not rule out differences in the staining sensitivity among the individual species within the broad flow cytometry-based groups. Also at some stations, the total event count in dead controls was much higher than in non-heated samples which further complicates the interpretation of dead controls. If we exclude these stations and assume that the heat treatment is fatal to all phytoplankton cells, then an average of 12% of the dead phytoplankton would not express SYTOX Green fluorescence when killed by heat treatment. If this staining anomaly carries on to natural environment and other causes of death, then our analysis slightly overestimates the viability. This overestimation would generally be low, and because there are no clear trends between staining of heat-killed cells and the abundance ratios of the phytoplankton groups, we argue that the lower viability of G3 is a true observation and not entirely caused by differences in staining sensitivity. The positive relationship between viability in heat-treated samples and the Chl *a* concentration might be a more serious source of error with our method. This suggests that the SYTOX Green concentration we used was not sufficient to stain all the phytoplankton in dead controls when their density was high, which might lead to lower fluorescence intensity and thus to overestimation of viability in such situations. Viabilities $> 15\%$ in dead controls started to appear when the Chl *a* concentration was > 8 µg L^{-1} although also low viability values persisted with such high Chl *a* concentrations. This possible overestimation of viability cannot be proven nor removed retrospectively. Instead we emphasize the uncertainty of viability estimates at high Chl *a* concentrations and suggest SYTOX Green concentration to be adapted to Chl *a* concentration.

Our results are in line with other studies that report high variability in phytoplankton viabilities among different phytoplankton taxa (e.g. Veldhuis et al. 2001; Hayakawa et al. 2008; Rychtecký et al. 2014). Hayakawa et al. (2008) quantified phytoplankton viability with an enzymatic membrane permeability test and found that eukaryotic phytoplankton (< 10 µm) had significantly lower viability compared to *Synechococcus* sp. in the northwest Pacific Ocean. Also, Veldhuis et al. (2001) found the highest percentages of viable cells in *Synechococcus* sp., with a viability range of 75–95% during spring. Similarly, in our study, the viability of picocyanobacteria (G1), mainly represented by *Synechococcus* spp. in the Baltic Sea (Kuosa 1991; Motwani and Gorokhova 2013), varied from 77 to 91%. However, Peperzak and Brussaard (2011) reported poor staining by SYTOX Green of *Synechococcus* sp. If *Synechococcus* sp. globally stain poorly with SYTOX Green and, as a result, the green fluorescence intensity of some dead *Synechococcus* sp. cells stays below the five times background fluorescence of the sample, then it is possible that the viabilities reported for G1 in this study are overestimated. Also G2 and G3 might contain significant amounts of phytoplankton species with poor staining response to SYTOX Green. This is an inherent limitation of SYTOX Green method and with our data we cannot assess the responses of individual species included in the flow cytometry-based phytoplankton groups. Yet, SYTOX Green is a commonly used viability probe, which functioned well with most of the species tested by Peperzak and

Brussaard (2011) including small local species such as *Rhodomonas baltica*, and we assume that our results are comparable with other studies investigating phytoplankton viability at the community level.

The depth-dependent variation in viability could possibly be explained by stratification of the water column. G2 viability at 60 m (18 stations) was slightly higher at stations where the halocline was deeper and the 60 m sample was retrieved above the halocline. Temperature above the halocline was mostly uniform suggesting that the water column above the halocline was well mixed at most stations. This may result in uniform average viability of the phytoplankton when the cells are retained within the mixed layer and assumed to be regularly brought into the photic layer. However, the photic layer was always much shallower than the halocline (minimum distance between euphotic zone and upper limit of halocline varied between 15 and 64 m). Thus, phytoplankton may be exposed to extended periods of darkness even within the mixed layer, which may explain the decreased G2 viability in the deep end of the mixed layer (most 30 m measurements). If the cells end up below the mixed layer (as seen in 8 out of 16, 60 m depth measurements), and therefore permanently beyond the photic zone and the compensation depth, even higher decrease in viability could be expected, as was seen for all flow cytometry-based phytoplankton groups. Any changes in viability caused by light intensity (Agustí 2004) could therefore be expected to be influenced by the mixed layer depth.

We detected lower abundances of all flow cytometry-based phytoplankton groups in the warmer southern stations compared to the sampling sites in the north (Table 2). In addition, our regression models suggest a negative relationship between temperature and G2 abundance (Fig. 6c) which indicates that phytoplankton might encounter higher grazing pressure in warmer waters where growth rate of zooplankton is higher (Sommer et al. 2007). Higher grazing pressure in the south could also be suggested based on the anomalous spatial distribution of G1 (including *Synechococcus* spp.) in our study area. In general, even the cold-adapted clades of *Synechococcus* spp. are more abundant in warmer waters (Paulsen et al. 2016), but in our study, G1 (including *Synechococcus* spp.) had the highest abundance in the colder northern Baltic Sea and was either low or absent at most of the stations in the south, which could be an indication of top down control.

Nutrient limitation (Agustí 2004; Alonso-Laita and Agustí 2006; Rychtecký et al. 2014) and temperature (Alonso-Laita and Agustí 2006) have been shown to determine phytoplankton viability in the field. At many stations in the BP, the NO_3^- concentration was not detectable, indicating that the phytoplankton community had already consumed most of the NO_3^- available and entered an N-limited physiological state. In our results, the only correlation between abiotic factors and viable cells was the weak correlation between PO_4^{3-} concentration and G2 viability implying a decoupling between nutrient concentration and viability. Somewhat surprisingly, G2 abundance correlated negatively with PO_4^{3-} concentration (Fig. 6b). Concurrently, G3 abundance correlated positively with NH_4^+ concentration (Fig. 6a), but G3 viability did not. It seems, therefore, that the environmental variables controlling phytoplankton abundance cannot directly be used to predict phytoplankton viability. For example, abundance may be affected by grazing and sinking, whereas viability might not. However, there is uncertainty in the regression analysis involving $NH4^+$ concentration, because at some stations the measured concentrations were below the accurate detection limit.

Our results demonstrate that inorganic nutrient concentration cannot per se be used to evaluate the physiological state of phytoplankton, even though phosphate concentration seemed to explain a small fraction of the variation in G2 viability. Nutrient affinity is tightly linked to size as the surface to volume ratio changes with a 2/3 power exponent, and the smaller sized picophytoplankton satisfy their nutritional needs at a much lower nutrient concentration (Irwin et al. 2006). In addition, with rapid nutrient turnover, the phytoplankton cells might not experience nutrient stress even at very low inorganic nutrient concentrations. This might in part explain the high G2 abundance in low PO_4^{3-}concentration, as especially the small phytoplankton gain competitive advantage against larger cells by efficiently using the recycled PO_4^{3-} in nutrient depleted environment (Irwin et al. 2006). The photochemical efficiency (F_v/F_m) is a better proxy for physiological state as the photosynthesis is rapidly downregulated during stress conditions, e.g. depletion of inorganic nutrient(s), but there is also a taxonomic component affecting the F_v/F_m

(Suggett et al. 2009). In this study, F_v/F_m explained cell viability better than inorganic nutrient concentration. Especially G2 viability correlated with F_v/F_m (Fig. 6g), which could be due to their high abundance throughout the sampling area. A more comprehensive viability assessment of natural phytoplankton communities might reveal how well F_v/F_m and membrane integrity-based viability assessments are aligned. This, however, can be relatively complicated because as, e.g. Franklin et al. (2009) demonstrate, high F_v/F_m value might not be a clear sign of absence of dead cells, although cells with reduced viability likely have lower photosynthetic efficiency (Veldhuis et al. 2001). A drop in F_v/F_m might also be a transient response to stress, as phytoplankton continuously acclimates to their surroundings (Halsey and Jones 2015), and during the spring bloom in the Baltic Sea, the primary production output per Chl *a* unit (the assimilation number) is not affected by the inorganic nutrient concentration (Spilling et al. 2019). Therefore, it might be better to consider measurements of F_v/F_m and viability as complementary assays for the physiological state of phytoplankton communities. Also Veldhuis et al. (2001) coupled viability analyses with a photosynthetic stage measurement. By using ^{14}C incorporation as a determinant of cell physiological status, they found that populations of cells containing photopigments but possessing compromised membranes were, at least partially, capable of photosynthesis, but had lower ^{14}C fixation rates. Bulk measures such as ^{14}C fixation rates, while useful in overall population assessment, inevitably integrate physiological heterogeneity within microbial populations, meaning that correlations between the bulk measure, and single-cell measurement, are difficult to interpret (Davey and Kell 1996).

The question remains, what causes the presence of non-viable cells within the observed flow cytometry-based phytoplankton groups? Viability was occasionally fairly low even when Chl *a* concentration was high. This was especially pronounced at the station LL7S during both samplings, where Chl *a* was exceptionally high (23.5 and 26.1 µg L^{-1} on the first and the second sampling, respectively), but the viability of each flow cytometry-based group was comparable to stations with lower Chl *a* concentration. One possible explanation could be the allelopathic interactions among the members of the microbial community. Among such interactions is the release of PUAs, which have been shown to induce cell death among some phytoplankton species (Ribalet et al. 2007). PUAs can be produced by different phytoplankton species, but especially by diatoms. For example, Taylor et al. (2009) observed increased PUA production in *Skeletonema marinoi* during increased nutrient limitation in spring in the Baltic Sea. *Skeletonema marinoi* was not present in high numbers during the cruise, but at many stations diatom abundance was high (up to 5000 cells mL^{-1}), and there was a clear negative correlation between total diatom biomass and G2 viability (Fig. 6e) which might indicate allelopathy, possibly mediated by PUAs. However, this interpretation is complicated by the low diatom biomass at several stations and by the positive correlation between diatom biomass and G2 abundance (Fig. 6d). A possible explanation for this observed conflict could be that the conditions were favourable for growth of both G2 and diatoms and PUA production started only at high cell densities at the onset of diatom bloom decline, as has been demonstrated for *S. marinoi* by Vidoudez et al. (2011b). Cózar et al. (2018) concluded, based on in situ measurements, that per cell release of PUAs increases with increased oligotrophy, presumably to enhance the bacterial remineralization rates of nutrients (Edwards et al. 2015). Most of the Baltic Sea is far from oligotrophic, but towards the end of the bloom the nutrient limitation might induce an increase in PUA production, which, given the high phytoplankton density, could result in a sufficiently high PUA concentration to induce a detectable reduction in viability in the measured fraction of the phytoplankton population. Since G2 viability also correlated negatively with the total abundance of flow cytometry-based phytoplankton (Fig. 6f), we cannot rule out the possibility of PUA mediated allelopathy among the small phytoplankton (Vidoudez et al. 2011a; Morillo-García et al. 2014). However, without measurements of PUA concentrations this remains speculation.

Dead phytoplankton cells have emerged as an important DOC source in many, mainly oligotrophic, marine environments (e.g. Kirchman 1999; Franklin et al. 2006; Agustí and Duarte 2013). In coastal seas, such as the Baltic Sea, autochthonous DOC from riverine sources may account for a substantial part of the DOC pool (Hoikkala et al. 2012). The Baltic Sea has various dissolved organic matter sources, and the influence of allochthonous DOC is strong (Sandberg

et al. 2004; Alling et al. 2008; Kuliński and Pempkowiak 2008). Terrestrial origin of DOC could have been important also during our study, as we did not detect a relationship between viability and DOC. DOC concentration correlated slightly positively with G3 abundance (Fig. 6h) indicating that they might have produced a detectable increase in the DOC pool. This relationship was mainly caused by the two very high DOC values at LL7S and LL9 and was not significant anymore if these stations were excluded. Yet, these values are within the natural variation of DOC concentration in the area and were included in the analysis. Viability of G3 was on average lower than the viability of G2 which would support an interpretation that dying cells contribute to the DOC pool. However, the abundance of G3 was very low throughout the cruise; G2 was often 10 times more abundant and many large phytoplankton, such as large diatoms and dinoflagellates, which likely have been excluded from the flow cytometry-based G3 category, often coexisted in high abundances. With so low relative abundance, it seems unlikely that the DOC release from G3 would overshadow the DOC release from other, more abundant, phytoplankton groups. Our results therefore suggest that sources other than cell death might be more important for the DOC concentration, although DOC release from dying larger phytoplankton (Camarena-Gómez et al. 2018) cannot be excluded with our viability data that concentrated in the smaller size fractions. DOC may also originate from living phytoplankton (Thornton 2014) through passive diffusion (Bjørrisen 1988) or active release (Wear et al. 2015), or from heterotrophs (Steinberg and Landry 2017).

Conclusions

Essential complementary information on phytoplankton communities can be acquired by flow cytometry to address important ecological questions such as the distribution and fate of microalgal cells. By investigating the spatial patterns of phytoplankton viability and separately the different groups identified by flow cytometry, this study contributes to filling the gap of knowledge on the physiological condition of the phytoplankton communities across the Baltic Sea. We demonstrated that viability in natural phytoplankton communities in the Baltic Sea varied among different functional groups, and that non-viable cells were always present. Cell death therefore contributes to spring bloom dynamics where grazing and sinking traditionally have been regarded as the main loss factors. We found that abiotic factors that affect the viability of phytoplankton communities in other marine environments may not be as clearly associated with phytoplankton viability in the Baltic Sea during spring. We also showed that factors affecting the abundance of phytoplankton were not the same factors that affected their viability. Further studies assessing viability of larger phytoplankton taxa during other seasons are needed to understand their role in contributing to the Baltic Sea DOC pool.

Acknowledgements Open access funding provided by University of Helsinki including Helsinki University Central Hospital. This study was funded by the Walter and Andrée de Nottbeck Foundation (MV, SE, TT), the Swedish Cultural Foundation in Finland (TT), and Academy of Finland (KS, decision no 259164). The study utilized SYKE marine research infrastructure as a part of the national FINMARI consortium. We kindly thank the crew and scientific staff of R/V Aranda for their support during the CFLUX16 cruise and Johanna Oja for doing the microscopy counts.

Compliance with ethical standards

Conflict of interest The authors declare that they have no conflict of interest.

References

Agustí S (2004) Viability and niche segregation of *Prochlorococcus* and *Synechococcus* cells across the Central Atlantic Ocean. Aquat Microb Ecol 36:53–59

Agustí S, Duarte CM (2000) Strong seasonality in phytoplankton cell lysis in the NW Mediterranean littoral. Limnol Oceanogr 45:940–947

Agustí S, Duarte CM (2013) Phytoplankton lysis predicts dissolved organic carbon release in marine plankton communities. Biogeosciences 10:1259–1264

Agustí S, Sánchez MC (2002) Cell viability in natural phytoplankton communities quantified by a membrane permeability probe. Limnol Oceanogr 47:818–828

Alling V, Humborg C, Mörth CM, Rahm L, Pollehne F (2008) Tracing terrestrial organic matter by $\delta^{34}S$ and $\delta^{13}C$ signatures in a subarctic estuary. Limnol Oceanogr 53:2594–2602

Alonso-Laita P, Agustí S (2006) Contrasting patterns of phytoplankton viability in the subtropical NE Atlantic Ocean. Aquat Microb Ecol 43:67–78

Benner R, Von Bodungen B, Farrington J, Hedges J, Lee C, Mantoura F, Suzuki Y, Williams PM (1993) Measurement of dissolved organic carbon and nitrogen in natural waters: workshop report. Mar Chem 41:5–10

Berges JA, Falkowski PG (1998) Physiological stress and cell death in marine phytoplankton: induction of proteases in response to nitrogen or light limitation. Limnol Oceanogr 43:129–135

Berman-Frank I, Bidle KD, Haramaty L, Falkowski PG (2004) The demise of the marine cyanobacterium, Trichodesmium spp., via an autocatalyzed cell death pathway. Limnol Oceanogr 49:997–1005

Bidle KD (2015) The molecular ecophysiology of programmed cell death in marine phytoplankton. Annu Rev Mar Sci 7:341–375

Bidle KD, Falkowski PG (2004) Cell death in planktonic, photosynthetic microorganisms. Nat Rev Microbiol 2(8):643

Bjørrisen PK (1988) Phytoplankton exudation of organic matter: why do healthy cells do it? Limnol Oceanogr 33:151–154

Bramucci AR, Case RJ (2019) Phaeobacter inhibens induces apoptosis-like programmed cell death in calcifying *Emiliana huxleyi*. Sci Rep 9(1):5215

Brussaard CPD, Riegman R, Noordeloos AAM, Cadée GC, Witte H, Kop AJ, Nieuwland G, van Duyl FC, Bak RPM (1995) Effects of grazing, sedimentation and phytoplankton cell lysis on the structure of a coastal pelagic food web. Mar Ecol Prog Ser 123:259–271

Camarena-Gómez MT, Lipsewers T, Piiparinen J, Eronen-Rasimus E, Perez-Quemaliños D, Hoikkala L, Sobrino C, Spilling K (2018) Shifts in phytoplankton community structure modify bacterial production, abundance and community composition. Aquat Microb Ecol 81:149–170

Casotti R, Mazza S, Brunet C, Vantrepotte V, Ianora A, Miralto A (2005) Growth inhibition and toxicity of the algal aldehyde 2-trans-2-cis decadienal on *Thalassiosira weissflogii* (Bacillariophyceae). J Phycol 41:7–20

Cózar A, Morillo-García S, Ortega MJ, Li QP, Bartual A (2018) Macroecological patterns of the phytoplankton production of polyunsaturated aldehydes. Sci Rep 8:12282

Davey HM, Kell DB (1996) Flow cytometry and cell sorting of heterogeneous microbial populations: the importance of single-cell analyses. Microbiol Mol Biol Rev 60(4):641–696

Edwards BR, Bidle KD, Van Mooy BAS (2015) Dose-dependent regulation of microbial activity on sinking particles by polyunsaturated aldehydes: implications for the carbon cycle. Proc Natl Acad Sci USA 112:5909–5914

Fleming-Lehtinen V, Laamanen M, Kuosa H, Haahti H, Olsonen R (2008) Long-term development of inorganic nutrients and chlorophyll a in the open northern Baltic Sea. Ambio 37:86–93

Franklin DJ, Brussaard CPD, Berges JA (2006) What is the role and nature of programmed cell death in phytoplankton ecology? Eur J Phycol 41:1–14

Franklin DJ, Choi CJ, Hughes C, Malin G, Berges JA (2009) Effect of dead phytoplankton cells on the apparent efficiency of photosystem II. Mar Ecol Prog Ser 382:35–40

Gallo C, d'Ippolito G, Nuzzo G, Sardo A, Fontana A (2017) Autoinhibitory sterol sulfates mediate programmed cell death in a bloom-forming marine diatom. Nat Commun 8(1):1292

Grasshoff K, Ehrhardt M, Kremling K (1983) Methods of seawater analysis. Verlag Chemie, Weinheim

Gustafsson EW, Deutsch B, Gustafsson BG, Humborg C, Mörth CM (2014) Carbon cycling in the Baltic Sea—the fate of allochthonous organic carbon and its impact on air–sea CO_2 exchange. J Mar Syst 129:289–302

Halsey KH, Jones BM (2015) Phytoplankton strategies for photosynthetic energy allocation. Ann Rev Mar Sci 7:265–297

Hayakawa M, Suzuki K, Saito H, Takahashi K, Ito SI (2008) Differences in cell viabilities of phytoplankton between spring and late summer in the northwest Pacific Ocean. J Exp Mar Biol Ecol 360:63–70

Hoikkala L, Lahtinen T, Perttilä M, Lignell R (2012) Seasonal dynamics of dissolved organic matter on a coastal salinity gradient in the northern Baltic Sea. Cont Shelf Res 45:1–14

Hoikkala L, Kortelainen P, Soinne H, Kuosa H (2015) Dissolved organic matter in the Baltic Sea. J Mar Syst 142:47–61

Irwin AJ, Finkel ZV, Schofield OM, Falkowski PG (2006) Scaling-up from nutrient physiology to the size-structure of phytoplankton communities. J Plankton Res 28:459–471

Jespersen AM, Christoffersen K (1987) Measurements of chlorophyll *a* from phytoplankton using ethanol as extraction solvent. Arch Hydrobiol 109:445–454

Jiménez C, Capasso JM, Edelstein CL, Rivard CJ, Lucia S, Breusegem S, Berl T, Segovia M (2009) Different ways to die: cell death modes of the unicellular chlorophyte *Dunaliella viridis* exposed to various environmental stresses are mediated by the caspase-like activity DEVDase. J Exp Bot 60:815–828

Kahru M, Elmgren R, Savchuk OP (2016) Changing seasonality of the Baltic Sea. Biogeosciences 13:1009–1018

Kirchman DL (1999) Phytoplankton death in the sea. Nature 398:293–294

Kuliński K, Pempkowiak J (2008) Dissolved organic carbon in the southern Baltic Sea: quantification of factors affecting its distribution. Estuar Coast Shelf Sci 78:38–44

Kuosa H (1991) Picoplanktonic algae in the northern Baltic Sea: seasonal dynamics and flagellate grazing. Mar Ecol Prog Ser 73:269–276

Li WKW, McLaughlin FA, Lovejoy C, Carmack EC (2009) Smallest algae thrive as the Arctic Ocean freshens. Science 326:539

Lignell R, Heiskanen A-S, Kuosa H, Gundersen K, Kuuppo-Leinikki P, Pajuniemi R, Uitto A (1993) Fate of a phytoplankton spring bloom: sedimentation and carbon flow in the planktonic food web in the northern Baltic. Mar Ecol Prog Ser 94:239–252

Lipsewers T, Spilling K (2018) Microzooplankton, the missing link in Finnish plankton monitoring programs. Boreal Environ Res 23:127–137

Llabrés M, Agustí S (2006) Picophytoplankton cell death induced by UV radiation: evidence for oceanic Atlantic communities. Limnol Oceanogr 51:21–29

Luhtala H, Tolvanen H (2013) Optimizing the use of secchi depth as a proxy for euphotic depth in coastal waters: an empirical study from the Baltic Sea. ISPRS Int J Geo Inf 2(4):1153–1168

Menden-Deuer S, Lessard EJ (2000) Carbon to volume relationships for dinoflagellates, diatoms, and other protist plankton. Limnol Oceanogr 45:569–579

Morillo-García S, Valcárcel-Pérez N, Cózar A, Ortega MJ, Macías D, Ramírez-Romero E, García CM, Echevarría F, Bartual A (2014) Potential polyunsaturated aldehydes in the strait of Gibraltar under two tidal regimes. Mar Drugs 12:1438–1459

Motwani NH, Gorokhova E (2013) Mesozooplankton grazing on picocyanobacteria in the Baltic Sea as inferred from molecular diet analysis. PLoS One 8:e79230

Olenina I, Hajdu S, Edler L, Andersson A, Wasmund N, Busch S, Göbel J, Gromisz S, Huseby S, Huttunen M, Jaanus A, Kokkonen P, Ledaine I, Niemkiewicz E (2006) Biovolumes and size-classes of phytoplankton in the Baltic Sea. Balt Sea Environ Proc 106. HELCOM, Helsinki, pp 142

Olson RJ, Zettler ER, DuRand MD (1993) Phytoplankton analysis using flow cytometry. In: Kemp PF et al (eds) Handbook of methods in aquatic microbial ecology. CRC Press, Florida

Packard T, Chen W, Blasco D, Savenkoff C, Vézina AF, Tian R, St-Amand L, Roy SO, Lovejoy C, Klein B, Therriault JC, Legendre L, Ingram RG (2000) Dissolved organic carbon in the Gulf of St. Lawrence. Deep Sea Res Pt II 47:435–459

Paulsen ML, Doré H, Garczarek L, Seuthe L, Muller O, Sandaa R-A, Bratbak G, Larsen A (2016) *Synechococcus* in the Atlantic gateway to the Arctic ocean. Front Mar Sci 3:191

Peperzak L, Brussaard CPD (2011) Flow cytometric applicability of fluorescent vitality probes on phytoplankton. J Phycol 47:692–702

R Core Team (2018) R: a language and environment for statistical computing. R Foundation for Statistical Computing, Vienna. https://www.R-project.org/. Accessed 1 Sept 2018

Ribalet F, Berges JA, Ianora A, Casotti R (2007) Growth inhibition of cultured marine phytoplankton by toxic algal-derived polyunsaturated aldehydes. Aquat Toxicol 85:219–227

Ribalet F, Bastianini M, Vidoudez C, Acri F, Berges J, Ianora A, Miralto A, Pohnert G, Romano G, Wichard T, Casotti R (2014) Phytoplankton cell lysis associated with polyunsaturated aldehyde release in the Northern Adriatic Sea. PLoS One 9:e85947

Rychtecký P, Znachor P, Nedoma J (2014) Spatio-temporal study of phytoplankton cell viability in a eutrophic reservoir using SYTOX green nucleic acid stain. Hydrobiologia 740:177–189

Saba GK, Steinberg DK, Bronk DA (2011) The relative importance of sloppy feeding, excretion, and fecal pellet leaching in the release of dissolved carbon and nitrogen by *Acartia tonsa* copepods. J Exp Mar Biol Ecol 404:47–56

Sandberg J, Andersson A, Johansson S, Wikner J (2004) Pelagic food web structure and carbon budget in the northern Baltic Sea: potential importance of terrigenous carbon. Mar Ecol Prog Ser 268:13–29

Schieler BM, Soni MV, Brown CM, Coolen MJL, Fredricks H, Van Moon BAS, Hirsh DJ, Bidle KD (2019) Nitric oxide production and antioxidant function during viral infection of the coccolithophore *Emiliana huxleyi*. ISME J 13:1019–1031

Smith SR (2009) Flow cytometric analysis of phytoplankton viability in Elkhorn Slough, California. MSc thesis. San Jose State University, San Jose

Sommer U, Aberle N, Engel A, Hansen T, Lengfellner K, Sandow M, Wohlers J, Zöllner E, Riebesell U (2007) An indoor mesocosm system to study the effect of climate change on the late winter and spring succession of Baltic Sea phyto- and zooplankton. Oecologia 150:655–667

Spilling K, Olli K, Lehtoranta J, Kremp A, Tedesco L, Tamelander T, Klais K, Peltonen H, Tamminen T (2018) Shifting diatom—dinoflagellate dominance during spring bloom in the Baltic Sea and its potential effects on biogeochemical cycling. Front Mar Sci 5:327

Spilling K, Fuentes-Lema A, Quemaliños D, Klais R, Sobrino C (2019) Primary production, carbon release, and respiration during spring bloom in the Baltic Sea. Limnol Oceanogr 64:1779–1789

Steinberg DK, Landry MR (2017) Zooplankton and the carbon cycle. Annu Rev Mar Sci 9:413–444

Suggett DJ, Moore CM, Hickman AE, Geider RJ (2009) Interpretation of fast repetition rate (FRR) fluorescence: signatures of phytoplankton community structure versus physiological state. Mar Ecol Prog Ser 376:1–19

Tamelander T, Spilling K, Winder M (2017) Organic matter export to the seafloor in the Baltic Sea: drivers of change and future projections. Ambio 46:842–851

Tarran GA, Bruun JT (2015) Nanoplankton and picoplankton in the Western English Channel: abundance and seasonality from 2007–2013. Prog Oceanogr 137:446–455

Taylor RL, Abrahamsson K, Godhe A, Wängberg SÅ (2009) Seasonal variability in polyunsaturated aldehyde production among strains of *Skeletonema marinoi* (Bacillariophyceae). J Phycol 45:46–53

Thornton DCO (2014) Dissolved organic matter (DOM) release by phytoplankton in the contemporary and future ocean. Eur J Phycol 49(1):20–46

Timmermans KR, Veldhuis MJW, Brussaard CPD (2007) Cell death in three marine diatom species in response to different irradiance levels, silicate, or iron concentrations. Aquat Microb Ecol 46:253–261

Utermöhl H (1958) Zur Vervollkommnung der quantitativen phytoplankton-methodik. Mitteilungen der Internationale Vereinigung für Theoretische und Angewandte. Limnologie 9:1–38

Veldhuis MJW, Kraay GW, Timmermans KR (2001) Cell death in phytoplankton: correlation between changes in membrane permeability, photosynthetic activity, pigmentation and growth. Eur J Phycol 36:167–177

Vidoudez C, Casotti R, Bastianini M, Pohnert G (2011a) Quantification of dissolved and particulate polyunsaturated aldehydes in the Adriatic Sea. Mar Drugs 9:500–513

Vidoudez C, Nejstgaard JC, Jakobsen HH, Pohnert G (2011b) Dynamics of dissolved and particulate polyunsaturated

aldehydes in mesocosms inoculated with different densities of the diatom *Skeletonema marinoi*. Mar Drugs 9:345–358

Wear EK, Carlson CA, James AK, Brzezinski MA, Windecker LA, Nelson CE (2015) Synchronous shifts in dissolved organic carbon bioavailability and bacterial community responses over the course of an upwelling-driven phytoplankton bloom. Limnol Oceanogr 60:657–677

Zuur AF, Ieno EN, Elphick CS (2010) A protocol for data exploration to avoid common statistical problems. Methods Ecol Evol 1:3–14